Singapore Management University

Institutional Knowledge at Singapore Management University

Research Collection School Of Computing and Information Systems

School of Computing and Information Systems

4-1995

An upper limit for the τ neutrino mass from τ → 5π(π0)ντ decays

D. BUSKULIC

M. THULASIDAS
Singapore Management University, manojt@smu.edu.sg

Follow this and additional works at: https://ink.library.smu.edu.sg/sis_research

Part of the Databases and Information Systems Commons

Citation

1

An upper limit for the τ neutrino mass from $\tau \rightarrow 5\pi(\pi^0)\nu_\tau$ decays.

The ALEPH Collaboration*

Abstract

From a sample of 152,000 τ decays collected by the ALEPH detector at LEP an upper limit of 24 MeV at 95% CL on the τ neutrino mass has been determined. The limit is obtained using a two dimensional likelihood fit of the visible energy and the invariant mass distribution of 25 $\tau \rightarrow 5\pi(\pi^0)\nu_\tau$ events.

(To be submitted to Physics Letters B)

*See the following pages for the list of authors.

The ALEPH Collaboration

D. Buskulic, D. Casper, I. De Bonis, D. Decamp, P. Ghez, C. Goy, J.-P. Lees, M.-N. Minard, P. Odier, B. Pietrzyk

Laboratoire de Physique des Particules (LAPP), IN^{2}P^3-CNRS, 74019 Annecy-le-Vieux Cedex, France

F. Ariztizabal, M. Chmeissani, J.M. Crespo, I. Efthymiopoulos, E. Fernandez, M. Fernandez-Bosman, V. Gaitan, Ll. Garrido,[15] M. Martinez, S. Orteu, A. Pacheco, C. Padilla, F. Palla, A. Pascual, J.A. Perlas, F. Sanchez, F. Teubert

Institut de Fisica d'Altes Energies, Universitat Autonoma de Barcelona, 08193 Bellaterra (Barcelona), Spain[7]

D. Creanza, M. de Palma, A. Farilla, G. Iaselli, G. Maggi,[3] N. Marinelli, S. Natali, S. Nuzzo, A. Ranieri, G. Raso, F. Romano, F. Ruggieri, G. Selvaggi, L. Silvestris, P. Tempesta, G. Zito

Dipartimento di Fisica, INFN Sezione di Bari, 70126 Bari, Italy

X. Huang, J. Lin, Q. Ouyang, T. Wang, Y. Xie, R. Xu, S. Xue, J. Zhang, L. Zhang, W. Zhao

Institute of High-Energy Physics, Academia Sinica, Beijing, The People's Republic of China[8]

G. Bonvicini, D. Cassel,[28] M. Cattaneo, P. Comas, P. Coyle, H. Drevermann, A. Engelhardt, R.W. Forty, M. Frank, G. Ganis, M. Girone, R. Hagelberg, J. Harvey, R. Jacobsen,[24] P. Janot, B. Jost, J. Knobloch, I. Lehraus, M. Maggi, C. Markou,[27] E.B. Martin, P. Mato, H. Meinhard, A. Minten, R. Miquel, K. Moffeit,[29] P. Palazzi, J.R. Pater, P. Perrodo, J.-F. Pusztaszeri, F. Ranjard, L. Rolandi, D. Schlatter, M. Schmelling, W. Tejessy, I.R. Tomalin, R. Veenhof, A. Venturi, H. Wachsmuth, W. Wiedenmann, T. Wildish, W. Witzeling, J. Wotschack

European Laboratory for Particle Physics (CERN), 1211 Geneva 23, Switzerland

Z. Ajaltouni, M. Bardadin-Otwinowska,[2] A. Barres, C. Boyer, A. Falvard, P. Gay, C. Guicheney, P. Henrard, J. Jousset, B. Michel, S. Monteil, J-C. Montret, D. Pallin, P. Perret, F. Podlyski, J. Proriol, J.-M. Rossignol, F. Saadi

Laboratoire de Physique Corpusculaire, Université Blaise Pascal, IN^{2}P^3-CNRS, Clermont-Ferrand, 63177 Aubière, France

T. Fearnley, J.B. Hansen, J.D. Hansen, J.R. Hansen, P.H. Hansen, S.D. Johnson, B.S. Nilsson

Niels Bohr Institute, 2100 Copenhagen, Denmark[9]

A. Kyriakis, E. Simopoulou, I. Siotis, A. Vayaki, K. Zachariadou

Nuclear Research Center Demokritos (NRCD), Athens, Greece

A. Blondel,[21] G. Bonneaud, J.C. Brient, P. Bourdon, L. Passalacqua, A. Rougé, M. Rumpf, R. Tanaka, A. Valassi, M. Verderi, H. Videau

Laboratoire de Physique Nucléaire et des Hautes Energies, Ecole Polytechnique, IN^{2}P^3-CNRS, 91128 Palaiseau Cedex, France

D.J. Candlin, M.I. Parsons, E. Veitch

Department of Physics, University of Edinburgh, Edinburgh EH9 3JZ, United Kingdom[10]

E. Focardi, G. Parrini

Dipartimento di Fisica, Università di Firenze, INFN Sezione di Firenze, 50125 Firenze, Italy

M. Corden, M. Delfino,[12] C. Georgiopoulos, D.E. Jaffe

Supercomputer Computations Research Institute, Florida State University, Tallahassee, FL 32306-4052, USA [13,14]

A. Antonelli, G. Bencivenni, G. Bologna,[4] F. Bossi, P. Campana, G. Capon, F. Cerutti, V. Chiarella, G. Felici, P. Laurelli, G. Mannocchi,[5] F. Murtas, G.P. Murtas, M. Pepe-Altarelli, S. Salomone

Laboratori Nazionali dell'INFN (LNF-INFN), 00044 Frascati, Italy

P. Colrain, I. ten Have,[6] I.G. Knowles, J.G. Lynch, W. Maitland, W.T. Morton, C. Raine, P. Reeves, J.M. Scarr, K. Smith, M.G. Smith, A.S. Thompson, S. Thorn, R.M. Turnbull

Department of Physics and Astronomy, University of Glasgow, Glasgow G12 8QQ, United Kingdom[10]

U. Becker, O. Braun, C. Geweniger, G. Graefe, P. Hanke, V. Hepp, E.E. Kluge, A. Putzer, B. Rensch, M. Schmidt, J. Sommer, H. Stenzel, K. Tittel, M. Wunsch

Institut für Hochenergiephysik, Universität Heidelberg, 69120 Heidelberg, Fed. Rep. of Germany[16]

R. Beuselinck, D.M. Binnie, W. Cameron, D.J. Colling, P.J. Dornan, N. Konstantinidis, L. Moneta, A. Moutoussi, J. Nash, G. San Martin, J.K. Sedgbeer, A.M. Stacey

Department of Physics, Imperial College, London SW7 2BZ, United Kingdom[10]

G. Dissertori, P. Girtler, E. Kneringer, D. Kuhn, G. Rudolph

Institut für Experimentalphysik, Universität Innsbruck, 6020 Innsbruck, Austria[18]

C.K. Bowdery, T.J. Brodbeck, A.J. Finch, F. Foster, G. Hughes, D. Jackson, N.R. Keemer, M. Nuttall, A. Patel, T. Sloan, S.W. Snow, E.P. Whelan

Department of Physics, University of Lancaster, Lancaster LA1 4YB, United Kingdom[10]

A. Galla, A.M. Greene, K. Kleinknecht, J. Raab, B. Renk, H.-G. Sander, H. Schmidt, S.M. Walther, R. Wanke, B. Wolf

Institut für Physik, Universität Mainz, 55099 Mainz, Fed. Rep. of Germany[16]

J.J. Aubert, A.M. Bencheikh, C. Benchouk, A. Bonissent, G. Bujosa, D. Calvet, J. Carr, C. Diaconu, F. Etienne, M. Thulasidas, D. Nicod, P. Payre, D. Rousseau, M. Talby

Centre de Physique des Particules, Faculté des Sciences de Luminy, IN^{2}P^3-CNRS, 13288 Marseille, France

I. Abt, R. Assmann, C. Bauer, W. Blum, D. Brown,[24] H. Dietl, F. Dydak,[21] C. Gotzhein, A.W. Halley, K. Jakobs, H. Kroha, G. Lütjens, G. Lutz, W. Männer, H.-G. Moser, R. Richter, A. Rosado-Schlosser, A.S. Schwarz,[23] R. Settles, H. Seywerd, U. Stierlin,[2] R. St. Denis, G. Wolf

Max-Planck-Institut für Physik, Werner-Heisenberg-Institut, 80805 München, Fed. Rep. of Germany[16]

R. Alemany, J. Boucrot, O. Callot, A. Cordier, F. Courault, M. Davier, L. Duflot, J.-F. Grivaz, Ph. Heusse, M. Jacquet, D.W. Kim,[19] F. Le Diberder, J. Lefrançois, A.-M. Lutz, G. Musolino, I. Nikolic, H.J. Park, I.C. Park, M.-H. Schune, S. Simion, J.-J. Veillet, I. Videau

Laboratoire de l'Accélérateur Linéaire, Université de Paris-Sud, IN^{2}P^3-CNRS, 91405 Orsay Cedex, France

P. Azzurri, D. Abbaneo, G. Bagliesi, G. Batignani, S. Bettarini, U. Bottigli, C. Bozzi, G. Calderini, M. Carpinelli, M.A. Ciocci, V. Ciulli, R. Dell'Orso, I. Ferrante, F. Fidecaro, L. Foà,[1] F. Forti, A. Giassi, M.A. Giorgi, A. Gregorio, F. Ligabue, A. Lusiani, P.S. Marrocchesi, A. Messineo, G. Rizzo, G. Sanguinetti, A. Sciabà, P. Spagnolo, J. Steinberger, R. Tenchini, G. Tonelli,[26] G. Triggiani, C. Vannini, P.G. Verdini, J. Walsh

Dipartimento di Fisica dell'Università, INFN Sezione di Pisa, e Scuola Normale Superiore, 56010 Pisa, Italy

A.P. Betteridge, G.A. Blair, L.M. Bryant, Y. Gao, M.G. Green, D.L. Johnson, T. Medcalf, Ll.M. Mir, J.A. Strong

Department of Physics, Royal Holloway & Bedford New College, University of London, Surrey TW20 OEX, United Kingdom[10]

V. Bertin, D.R. Botterill, R.W. Clifft, T.R. Edgecock, S. Haywood, M. Edwards, P. Maley, P.R. Norton, J.C. Thompson

Particle Physics Dept., Rutherford Appleton Laboratory, Chilton, Didcot, Oxon OX11 OQX, United Kingdom[10]

B. Bloch-Devaux, P. Colas, H. Duarte, S. Emery, W. Kozanecki, E. Lançon, M.C. Lemaire, E. Locci, B. Marx, P. Perez, J. Rander, J.-F. Renardy, A. Rosowsky, A. Roussarie, J.-P. Schuller, J. Schwindling, D. Si Mohand, A. Trabelsi, B. Vallage

CEA, DAPNIA/Service de Physique des Particules, CE-Saclay, 91191 Gif-sur-Yvette Cedex, France[17]

R.P. Johnson, A.M. Litke, G. Taylor, J. Wear

Institute for Particle Physics, University of California at Santa Cruz, Santa Cruz, CA 95064, USA[22]

A. Beddall, C.N. Booth, R. Boswell, S. Cartwright, F. Combley, I. Dawson, A. Koksal, M. Letho, W.M. Newton, C. Rankin, L.F. Thompson

Department of Physics, University of Sheffield, Sheffield S3 7RH, United Kingdom[10]

A. Böhrer, S. Brandt, G. Cowan, E. Feigl, C. Grupen, G. Lutters, J. Minguet-Rodriguez, F. Rivera,[25] P. Saraiva, U. Schäfer, L. Smolik

Fachbereich Physik, Universität Siegen, 57068 Siegen, Fed. Rep. of Germany[16]

L. Bosisio, R. Della Marina, G. Giannini, B. Gobbo, L. Pitis, F. Ragusa[20]

Dipartimento di Fisica, Università di Trieste e INFN Sezione di Trieste, 34127 Trieste, Italy

H. Kim, J. Rothberg, S. Wasserbaech

Experimental Elementary Particle Physics, University of Washington, WA 98195 Seattle, U.S.A.

S.R. Armstrong, L. Bellantoni, P. Elmer, Z. Feng, D.P.S. Ferguson, Y.S. Gao, S. González, J. Grahl, J.L. Harton, O.J. Hayes, H. Hu, P.A. McNamara III, J.M. Nachtman, W. Orejudos, Y.B. Pan, Y. Saadi, M. Schmitt, I.J. Scott, V. Sharma, J.D. Turk, A.M. Walsh, F.V. Weber,[1] Sau Lan Wu, X. Wu, J.M. Yamartino, M. Zheng, G. Zobernig

Department of Physics, University of Wisconsin, Madison, WI 53706, USA[11]

1   Introduction

The question of a non-vanishing neutrino mass is of fundamental importance in particle physics. Furthermore the value of the τ neutrino mass has important cosmological implications. From cosmology the mass of a stable τ neutrino is bounded by its contribution to the energy density of the universe to be either smaller than $20 - 60$ eV or larger than $4 - 5$ GeV [1]. In the case of an unstable τ neutrino these constraints are no longer valid and the mass could be in the MeV range [2]. The presence of a neutrino with such a high mass could possibly be detected by experiments at e^+e^- colliders.

Direct limits on the tau neutrino mass have been derived by fitting the invariant mass spectrum of hadrons produced in tau decays with a likelihood technique. The lowest 95% CL limits have been obtained by ARGUS [3], 31 MeV with 20 $\tau \to 5\pi^\pm\nu_\tau$ events, and by CLEO II [4], 32.6 MeV with 60 $\tau \to 5\pi^\pm\nu_\tau$ and 53 $\tau \to 3\pi^\pm 2\pi^o\nu_\tau$ events.

In this letter an upper limit on the τ neutrino mass is presented, obtained with the ALEPH detector at LEP using a technique based on a two dimensional likelihood fit in the variables invariant mass and energy of the hadronic system in $\tau \to 5\pi^\pm(\pi^0)\nu_\tau$ decays. This method, recently applied by OPAL [5] to a 5 event sample, leads to a substantial gain in sensitivity with respect to the use of invariant mass alone.

2   The ALEPH Detector

The ALEPH detector is described in detail elsewhere [6]. A brief description of the elements of the apparatus relevant to the present analysis is given here.

Charged particles are tracked in an axial magnetic field of 1.5 T using a silicon vertex detector with two dimensional readout, a drift chamber and a time projection chamber (TPC). This combined tracking system provides up to 31 coordinates and up to 338 measurements of the specific ionization for each track.

For high momentum particles the transverse momentum resolution is $\Delta p_T/p_T = 6 \times 10^{-4} \ p_T$ GeV. The mass resolution for a multibody decay like $D^0 \to K^-\pi^-\pi^+\pi^+$ is typically 10 MeV.

Surrounding the tracking detectors are the electromagnetic calorimeter (ECAL), the superconducting solenoid, the hadron calorimeter (HCAL) and the muon chambers.

The ECAL is a lead wire-chamber calorimeter with cathode-pads read out in $0.9° \times 0.9°$ projective towers divided in three longitudinal segments, with an energy resolution of $\sigma_E/E = 0.18/\sqrt{E(GeV)} + 0.009$. The fine segmentation of the ECAL is fundamental for photon identification and π^0 reconstruction [7].

The HCAL is composed by 1.2 m of iron, interleaved with 23 layers of streamer tubes , while the muon chambers consist of two double layers of streamer tubes.

Charged particle (electron, muon, hadron) identification is performed with a likelihood method using the combined information of all subdetectors [8].

3   Event selection

This analysis is based on a data sample of 65 pb^{-1} collected by ALEPH in the years 1991, 1992 and 1993, which corresponds to 1.6 million hadronic events and 76,000 $\tau^+\tau^-$ pairs.

The data were selected using the standard ALEPH τ off-line filter [9] to isolate $e^+e^- \to \tau^+\tau^-$ events. Within the geometrical acceptance of 84.2% this selection has an average efficiency of 93.2% and a contamination from hadronic events of 0.25%.

The selected events were divided into two hemispheres by a plane perpendicular to the thrust axis and only events with at least one five prong hemisphere were retained. Each track in the event was required to have a momentum larger than 100 MeV, a polar angle greater than 18.2^0, to be reconstructed with at least 4 TPC coordinates, and to originate from a 2 cm radius 20 cm long cylinder around the nominal beam position. The five track system was required to have unit charge and $\sum_{i=1}^{5} |d_0| < 0.8$ cm, d_0 being the distance of closest approach to the interaction point in the plane perpendicular to the beam direction. Events with at least one of the five tracks identified as an electron or with a pair of tracks kinematically compatible with a photon conversion were rejected.

After applying the above cuts photon identification was performed in a 60° cone around the thrust axis. The photons were paired to form $\pi^0 s$ using a likelihood method which also rejects fake photons reconstructed near hadronic showers. Events with no photons were classified as 5π decays while events with two photons forming a π^0 candidate were classified as $5\pi\pi^0$. Any event with unpaired photons after π^0 reconstruction or with more than 1 π^0 candidate was rejected.

To suppress the contamination from $e^+e^- \to \tau\tau f\overline{f}$ events - hereafter referred to as four fermion events - and $e^+e^- \to q\overline{q}$ events some additional cuts were applied. The total invariant mass of the 5(6) pions was required to be smaller than 2.5 GeV. The charged multiplicity in the opposite hemisphere had to be smaller than 4. The invariant mass between charged tracks and photons of the opposite hemisphere was required to be smaller than the tau mass and the absolute value of the total charge of the event had to be smaller than 2.

The effects of these cuts on the selection efficiency are summarized in table 1. The $5\pi\pi^0$ mode has a smaller total efficiency because the dense hadronic activity in the ECAL masks the development of photon showers and consequently hinders π^0 reconstruction. According to Monte Carlo (MC) both efficiencies are independent of

Selection criteria	Signal modes	
	5π	$5\pi\pi^0$
$\tau^+\tau^-$ selection	75.89 ± 0.45	73.11 ± 0.46
5 prong selection	32.08 ± 0.46	27.22 ± 0.44
π^0 rejection/reconstruction	26.80 ± 0.44	7.70 ± 0.27
Additional cuts	24.71 ± 0.44	6.97 ± 0.25

Table 1: MC selection efficiency (in %) for the two signal modes after the different selection requirements.

the invariant mass (m_{had}), and of the energy (E_{had}) of the hadronic system.

After the selection 23 and 2 events were identified as 5π and $5\pi\pi^0$. Assuming the recent CLEO II measurement [10] of the branching fractions, 27 ± 3 and 3 ± 1 events were expected in the two channels. All the observed events are in the 5-1 topology. The position of several events on the E_{had} vs m_{had} plane is shown in Fig. 1. Only a part of this plane is kinematically accessible for the signal. The extent of the accessible region decreases with increasing neutrino mass. The allowed region is hereafter defined as the largest accessible region. Its border is drawn in Fig. 1 together with that corresponding to a 31 MeV massive neutrino. All but one of the selected events are inside the allowed region. The exception is a $5\pi\pi^0$ event, labeled 4 in Fig. 1, which is about one standard deviation away from the border.

4 The background

The effects of background on the determination of the limit on the neutrino mass depend strongly on the position in the E_{had} vs m_{had} plane of the background events and on the accuracy with which that position is determined. This is a consequence of the fact that the sensitivity to m_ν varies considerably across the plane, increasing near the border of the allowed region.

There are two kinds of background: misclassified τ decays which are reconstructed at a point in the plane with a different sensitivity to m_ν with respect to their true location, and non-$\tau^+\tau^-$ events which happen to lie inside or near the allowed region. In particular the addition of a fake particle to the true ones (like a fake π^0 to a $\tau \to 5\pi\nu_\tau$ decay) or the attribution to a particle of a larger mass (such as a conversion electron identified as a pion) can bias the determination of the limit on the neutrino mass to lower values. On the contrary misclassified tau decays in which a particle is lost (like an undetected π^0 in a $\tau \to 5\pi\pi^0\nu_\tau$ decay) bias the determination to higher values of the neutrino mass.

For this analysis the background is considered negligible either if it introduces a bias towards higher neutrino masses or if it contributes less than 1% to the total number of events entering a special 'sensitive' region of the plane defined as follows: given a distribution of events limiting the neutrino mass to 28 MeV at 95% CL the 'sensitive' region is that part of the plane where one extra event, with typical errors on m_{had} and E_{had} improves the limit by more than 1 MeV. The shape of the sensitive region is shown in Fig. 1. This shape does not depend on the specific distribution of the other events.

The number of background events predicted by the MC for the samples of the 5π and $5\pi\pi^0$ candidates is given in table 2 for both the whole plane and the sensitive region. The MC statistics employed in this evaluation amount to 10,000 $\tau \to 5\pi\nu_\tau$, 10,000 $\tau \to 5\pi\pi^0\nu_\tau$, 590,000 $e^+e^- \to \tau\tau$ events, 2.9 million $e^+e^- \to q\overline{q}$ events and 7500 four fermion events. The last three samples correspond respectively to 8 times, 2 times and 30 times the data statistics. A special production of hadronic events in the 5-1 configuration, equivalent to 6 million $q\overline{q}$ events, was also used.

Out of the two hadronic MC samples only one event from the 6 million sample

6

Background source	Signal Modes			
	5π		$5\pi\pi^0$	
	Full plane	Sensitive region	Full plane	Sensitive region
5π	-	-	0.15 ± 0.08	0.04 ± 0.03
$5\pi\pi^0$	1.0 ± 0.4	< 0.01	-	-
$K_s^0 K_s^0 \pi$	0.8 ± 0.4	0.1 ± 0.1	< 0.1	< 0.01
$3\pi\pi^0$	0.25 ± 0.18	< 0.01	0.13 ± 0.13	< 0.01
$q\overline{q}$	0.26 ± 0.26	< 0.01	< 0.3	< 0.01
$\tau^+\tau^- f\overline{f}$	0.05 ± 0.03	< 0.01	0.01 ± 0.01	< 0.01

Table 2: Background events expected in the selected samples from MC.

survives the selection being classified as a 5π event. It lies far from the border of the allowed region at low E_{had} value and shows an intense activity in the hadron calorimeter.

The background from four fermion events is composed mainly of $\tau^+\tau^-\mu^+\mu^-$ events where one of the taus decays in three prongs and forms together with the two muons the 5 prong system. The muons are not collinear with the tau and therefore the total mass is on average much higher than the tau mass. If the cut at $m_{had} < 2.5$ GeV were released one such event would in fact be observed in the data at $m_{had} = 17$ GeV. An additional tag for these events is the identification of the two muons. In the data sample only one out of 125 charged particles is identified as a muon, in agreement with the expectation from the $\pi \to \mu\nu_\mu$ decay rate inside the tracking volume and the misidentification probability.

The background from the misclassification of $3\pi\pi^0$ events is also very small. It originates from events in which the particle identification fails either because the electrons from a converted photon enter ECAL very close to an uninstrumented area, or because the momenta of the tracks are extremely low. The kinematic cuts to identify the conversions also fail in presence of a Dalitz decay of the π^0 or of a wrong measurement of the angular separation of the electrons. Their contribution is less important in the two dimensional approach because, although the invariant mass is overestimated, the total energy of the system is underestimated by the loss of one photon.

The $K_s^0 K_s^0 \pi$ contribution originates from K_s^0 decaying very close to the interaction point. As discussed later the decay dynamics of the 5 prong system affects very weakly the determination of the neutrino mass and hence $K_s^0 K_s^0 \pi$ events are not expected to bias the measurement.

The only non negligible background comes from the reciprocal contamination between 5π and $5\pi\pi^0$ decays. As stated before only 5π identified as $5\pi\pi^0$ can bias the limit on the neutrino mass to lower values. The possibility that $5\pi\pi^0$ events are in fact 5π decays has been considered in the evaluation of the systematics. The corresponding variation of the limit on the neutrino mass is small (~ 0.3 MeV).

In addition to the MC prediction the $q\overline{q}$ background has been determined directly from the data. Events in the 5-N topology were selected by applying the five prong

7

selection to the data without the $\tau^+\tau^-$ preselection and any of the additional cuts. This sample contains both signal and background events. Signal events can be anti-tagged to obtain a measurement of the background. The two hemispheres were treated independently and cuts on one of the two were used as tag for the opposite: requiring $N > 4$ the distribution of the background in the E_{had} vs m_{had} plane was measured; cutting at $m_{had} > 1.9$ GeV in the 5 prong hemisphere the distributions of N and of the invariant mass in the opposite hemisphere m_{opp} were determined.

Fig. 2 shows the distribution in the E_{had} vs m_{had} plane of the events selected with this procedure. The projections onto the two axes are in good agreement with the MC prediction, as are the distributions of N and m_{opp}.

Neglecting the correlations between the two hemispheres, it is possible to compute from the data the expected contamination, which is about 0.01 background events inside the sensitive region of which 0.006 in the 5-1 topology.

Finally by inspection of the topology in the opposite hemisphere of the events in the sensitive region (table 4) it appears that the interpretation of these events as originating from $Z \rightarrow q\bar{q}$ is even more unlikely.

5 The method

The limit on the mass is derived from an analytical maximum likelihood function giving the probability density of obtaining the observed distribution in the plane $(x = \frac{m_{had}}{m_\tau}, y = \frac{E_{had}}{E_{beam}})$.

For any given event i the probability density function $P_i(m_\nu)$ takes the form:

$$P_i(m_\nu) = \frac{1}{\mathcal{N}(m_\nu)} \int_{x_0}^{x_1(m_\nu)} dx \int_{m_\tau}^{E_{beam}} dE_\tau \mathcal{G}(E_\tau) \int_{y_0(E_\tau,m_\nu)}^{y_1(E_\tau,m_\nu)} dy \; \mathcal{R}(x-x_i, y-y_i)\epsilon(x,y)\frac{d^2\Gamma(x,y,m_\nu^2)}{dxdy}$$

Where :

- $\dfrac{d^2\Gamma(x,y,m_\nu^2)}{dxdy}$ is the theoretical distribution of the given decay mode;

- $\epsilon(x,y)$ is the selection efficiency;

- $\mathcal{R}(x - x_i, y - y_i)$ is the normalized resolution function, namely a multivariate Gaussian with an additional constant tail taking into account pattern recognition ambiguities in track reconstruction;

- $\mathcal{G}(E_\tau)$ is the initial state radiation function, derived from [11];

- $(y_0, y_1) = (\dfrac{E^*(1 - \beta\sqrt{1 - (\frac{m_{had}}{E^*})^2})}{m_\tau}, \dfrac{E^*(1 + \beta\sqrt{1 - (\frac{m_{had}}{E^*})^2})}{m_\tau})$,
  $E^* = \dfrac{m_\tau^2 + m_{had}^2 - m_\nu^2}{2m_\tau}$ being the hadronic energy in the τ rest frame and
  $\beta = \dfrac{p_\tau}{E_\tau}$ the τ velocity;

8

- $(x_0, x_1) = (\frac{\sum_{i=1}^{5(6)} m_\pi}{m_\tau}, \frac{m_\tau - m_\nu}{m_\tau})$;

- $\mathcal{N}(m_\nu)$ is the normalization factor.

The function $\frac{d^2\Gamma(x,y,m_\nu^2)}{dxdy}$ is defined only inside the allowed region. Consequently any event falling outside the allowed region contributes to the likelihood only to the extent permitted by the resolution function or by the radiation function.

The matrix elements of the decays of the two modes entering $\frac{d^2\Gamma(x,y,m_\nu^2)}{dxdy}$ are not presently fixed rigorously by any theory. This is because five pion decays are G odd and at best PCAC at low energy [12] could be invoked, while six pion decays involve a number of isospin amplitudes bigger than what can be determined via CVC from e^+e^- data [13]. Unlike other decays they are not dominated by a single low mass resonance and therefore a constant term has been used in the likelihood for the hadronic spectral functions ('phase space' approximation). Since spin 0 amplitudes are suppressed in τ decays, the hadronic system should contain at least two pions in a P wave, a ρ or an a_1 state. The use of intermediate ρ and a_1 production for the decay $\tau \to 5\pi\nu_\tau$ has been investigated convoluting a Breit-Wigner function with the appropriate phase space factors. In Fig. 3 the invariant mass spectrum is plotted for each different assumption while in Fig. 4 the mass spectra of the model without resonances and the a_1 model are compared to the data. The corresponding variations of the m_ν limit are small (~ 0.3 MeV) because near the kinematic limit the differences in the structure functions are washed out by the strong dependence of the phase space term on m_ν.

The statistics achievable near the end point depend strongly on the model as already shown by other tests performed with a $\rho\rho\pi$ model [14]. In the selected data sample five events are observed in the sensitive region. The probability of observing five or more events in this region is about 1% for the model without resonances and about 5% for the a_1 model.

The resolution functions $\mathcal{R}(x - x_i, y - y_i)$ have been investigated using the MC and checks have been performed on the data as explained in the next section. The resolutions in m_{had} and E_{had} can be well described using a Gaussian with a flat tail. The width of the Gaussian is 40% larger than what can be directly computed from the tracking and calorimetric errors. This effect is mainly due to pattern recognition ambiguities and it is correlated with the dense decay topology. The flat tail is due to the non-Gaussian nature of such errors and is unaffected by the presence of nuclear interactions. The fraction of events in the tails is on average 5%. The typical mass (energy) resolution for 5π events in the MC is 15 MeV (350 MeV) while for $5\pi\pi^0$ events is 35 MeV (800 MeV).

For every event the parameters of the resolution functions used in the fit were obtained from several hundred MC events, generated from the observed kinematic configuration as input. In a few cases small deviations of the average value of the reconstructed parameters from the input value were observed. These differences are taken into account in the systematics.

9

6   Results and systematic effects

Two fits have been performed, both converge to neutrino mass values compatible with zero: the one dimensional fit gives a 95% CL limit of 37.6 MeV and the two dimensional gives a limit of 23.0 MeV. The dependence of the likelihood on the neutrino mass is shown in Fig. 5 for both fits.

The above result has been corrected for systematics effects considering the following sources of uncertainty.

- Mass calibration and resolution: for the 5π events this has been investigated looking at the reconstructed D^0 mass in the decay chain $D^{*\,\pm} \to D^0\pi^{\pm}, D^0 \to K^-\pi^-\pi^+\pi^+$ where the energy of the D^* was required to be at least half the beam energy; the data are in agreement with the MC, giving an upper limit on the mass systematics of 0.5 MeV for the absolute value and a 20% increase for the resolution; the above values have been used in the evaluation of the systematics on the neutrino mass as shown in table 3 .

- Energy calibration: in both $J/\Psi \to \mu^+\mu^-$ and $D^0 \to K^-\pi^+$ decays the average opening angle between the daughter tracks is large (~ 200 mrad) so that the error on the reconstructed masses is dominated by the error on the energy; the data measurements are consistent with the expected values giving an upper limit on the energy systematics of $\Delta E = 2.7 \times 10^{-4}\ E\ (GeV)$. The systematics for the π^0 energy calibration have been estimated from $\tau \to \rho \to \pi\pi^0$ decays. A systematic uncertainty on the π^0 energy of 1% has been applied.

- Mass-Energy correlation: the average opening angle between the pions in $\tau \to 5\pi(\pi^0)\nu$ is relatively small ($\sim 50\ mrad$) so that the error on the mass receives a contribution also from the determination of the direction of the tracks. The average mass-energy correlation in MC is 54%. Conservatively the mass and energy systematics were considered to be 100% correlated.

- Resolution functions: the shape of the resolution functions has been computed event by event with the procedure described in the previous section. For few events small deviations from the input value of the mean reconstructed mass and energy were observed. These deviations have been introduced as a systematic error.

- τ mass: the value of the mass has been taken to be [15] $m_\tau = 1777.0 \pm 0.3$ MeV.

- Beam energy: uncertainties in beam energy determination have been investigated by the LEP calibration group [16]; an error of 6 MeV from the knowledge of the absolute beam energy has been applied to all events while a Gaussian error with a σ of 37 MeV from the beam energy spread has been applied separately to each event.

- Background: the effect of a possible background from 5π events classified as $5\pi\pi^0$ has been computed using a new likelihood where the probability density function

10

systematic source	variation	1d limit variation (MeV)	2d limit variation (MeV)
Mass offset	0.5 MeV	0.2	0.2
Energy offset	$0.027\%E$	-	0.2
Mass & energy offsets	100% correlation	-	0.3
Mass resolution	20%	2.0	0.2
π^0 energy resolution	1%	< 0.1	< 0.1
Resolution functions	Observed deviations	2.2	0.6
τ mass	0.3 MeV	0.3	0.2
E_{beam} calibration	6 MeV	-	0.1
E_{beam} spread	37 MeV	-	0.3
Background	5π class. $5\pi\pi^0$	0.2	0.3
total		3.0	0.8
Theoretical model	$\rho + 3\pi$	-0.3	-0.2
Theoretical model	$a_1 + 2\pi$	-0.5	-0.3

Table 3: Sources of systematic error and the resulting variation of the 95% CL limit on the τ neutrino mass.

of the jth $5\pi\pi^0$ event is redefined as $P'_{i=j} = 0.96\ P_j(5\pi\pi^0) + 0.04\ P_j(5\pi)$, thus ignoring the presence of the reconstructed π^0 with 4% weight. The variation of the limit on the neutrino mass was small ($\sim$ 0.3 MeV). The other sources of background are negligible and do not contribute to the systematics.

- τ lifetime: the effect of the lifetime on the tracking parameters within the MC has been found negligible for both the mass and the energy determination.

- Theoretical function: the limit on the neutrino mass is derived with the phase space approximation, the $\rho + 3\pi$ and $a_1 + 2\pi$ distributions give a result slightly smaller (by 0.2-0.3 MeV).

The systematic uncertainties and their effects on the fits are listed in table 3. The total systematic error is dominated by the knowledge of the resolution functions. Including the above effects the final result is then:

$$m_\nu \ <\ 40.6 \text{ MeV at 95\% CL for the one dimensional fit}$$

$$m_\nu \ <\ 23.8 \text{ MeV at 95\% CL for the two dimensional fit}$$

Finally the fit stability was investigated removing one event at the time from the fit. The result for the 5 events in the sensitive region is listed in table 4 together with the reconstructed τ decay in the opposite hemisphere.

7 Conclusions

A new upper limit on the τ neutrino mass of 24 MeV at 95% CL has been established determining detector effects and background contamination mostly from data. This

	1d limit variation (MeV)	2d limit variation (MeV)	τ decay opposite hemisphere
event 1	+8.8	+5.3	μ (20.0 GeV)
event 17	+6.8	+3.2	μ/h (1.3 GeV)
event 4	+1.2	+1.0	e (37.5 GeV)
event 14	+0.2	+2.3	h (5.5 GeV) + π^0 (9.0 GeV)
event 8	+0.8	+1.6	μ (3.8 GeV)

Table 4: Variation in the mass limit when one event is taken out of the fit. In the last column the reconstructed τ decay in the opposite hemisphere is reported together with the measured energy of the decay products.

value improves on the previous lowest limit of 31 MeV. The determination has benefited from a greater sensitivity to the neutrino mass obtained by using a two dimensional fitting procedure.

Acknowledgments

References

[1] H. Harari *et al.*, Nucl. Phys. B 292 (1987) 251

[2] G. Gyuk, M. Turner, Astroph-9410065 in *Neutrino 94*, Eilat, Israel (1994)

[3] ARGUS Collaboration, H. Albrecht et *al*, Phys. Lett. B 291 (1992) 221

[4] CLEO II Collaboration, D. Cinabro et *al*, Phys. Rev. Lett. 70 (1993) 3700

[5] OPAL Collaboration, R. Akers et *al*, CERN-PPE/94-107 (1994)

[6] ALEPH Collab., D. Decamp *et al.*, Nucl. Instr. Meth. A294 (1990) 121.

[7] ALEPH Collaboration, D. Buskulic *et al*, Zeit. fur Phys. C 59 (1993) 369

[8] ALEPH Collaboration, D. Decamp *et al*, Zeit. fur Phys. C 54 (1992) 211

[9] ALEPH Collaboration, D. Buskulic *et al*, Zeit. fur Phys. C 62 (1994) 539

[10] CLEO II Collaboration, D. Gibaut et *al*, Phys. Rev. Lett. 73 (1994) 934

[11] Z Physics at LEP 1, Vol. 1, CERN 89-08(1989), *Z line shape*

[12] Y. Tsai, Phys. Rev. D 4 (1971) 2621
     Y. Tsai, Phys. Rev. D 13 (1976) 771 (Erratum)

[13] A. Pais, Annals of Physics 9 (1960) 548

[14] J. J. Gomez-Cadenas *et al.*, Phys. Rev. D 41, 7 (1990) 2179

[15] Q. Nading, Proceedings of the Third Workshop on Tau Lepton Physics,
     Montreux, Switzerland (1994)

[16] The Working group on LEP Energy and the LEP Collaborations,
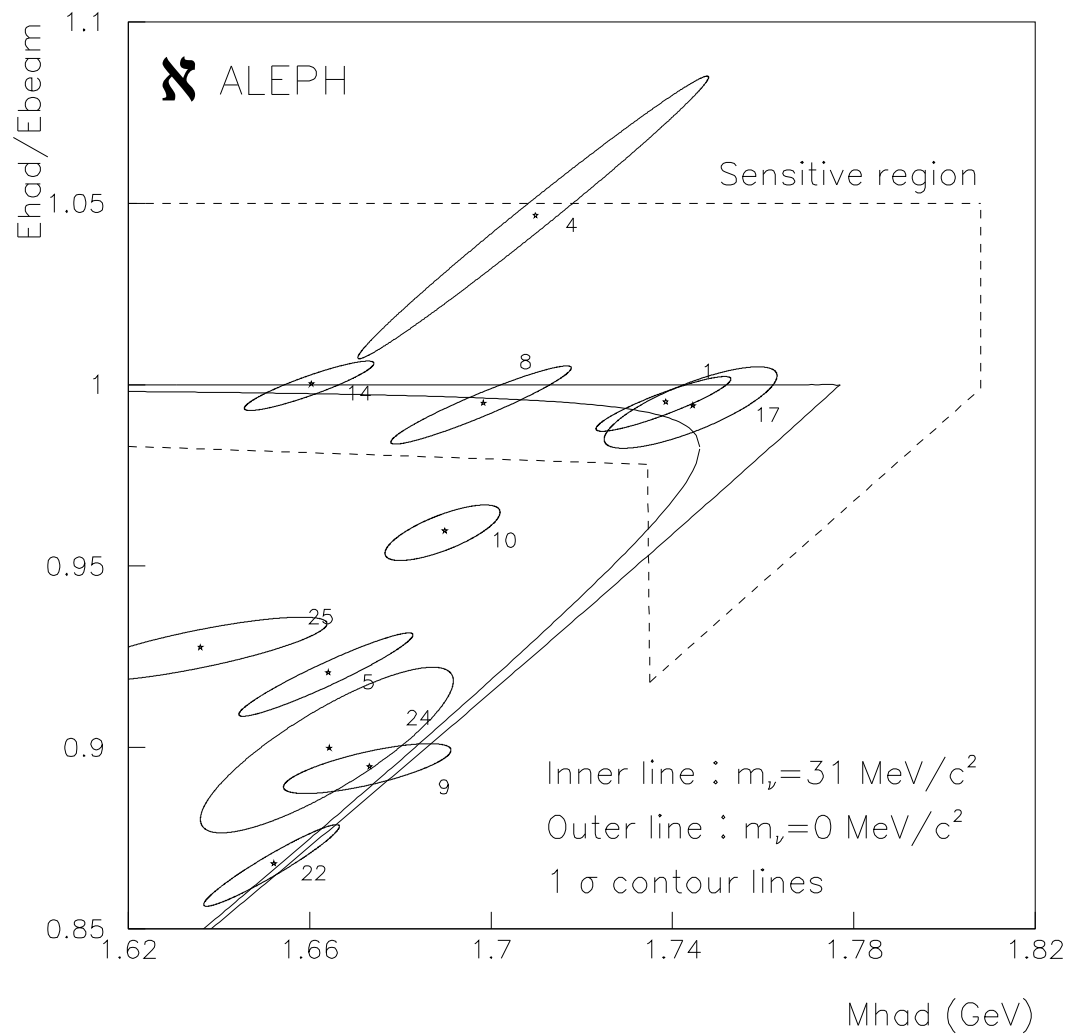   Phys. Lett.B 307 (1993) 187

Figure 1: Distribution of E_{had}/E_{beam} versus hadronic invariant mass of data events in the range $m_{had} > 1.62$ GeV and $E_{had}/E_{beam} > 0.85$. Events labeled 4 and 25 are identified as $\tau \to 5\pi\pi^0\nu_\tau$. The border of the sensitive region as defined in the text is also drawn (dashed line).
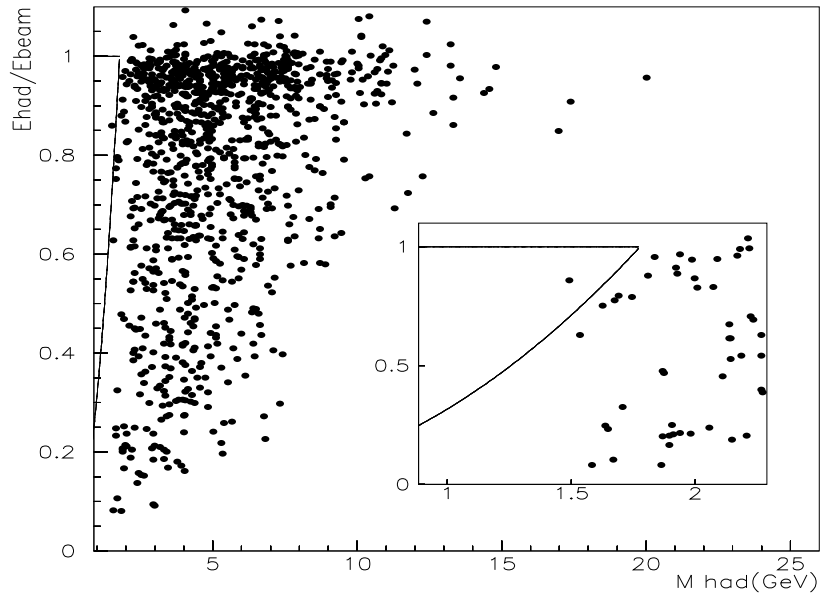
Figure 2: Distribution of E_{had}/E_{beam} versus hadronic invariant mass of non-$\tau^+\tau^-$ data events in the topology 5-N with N> 4.
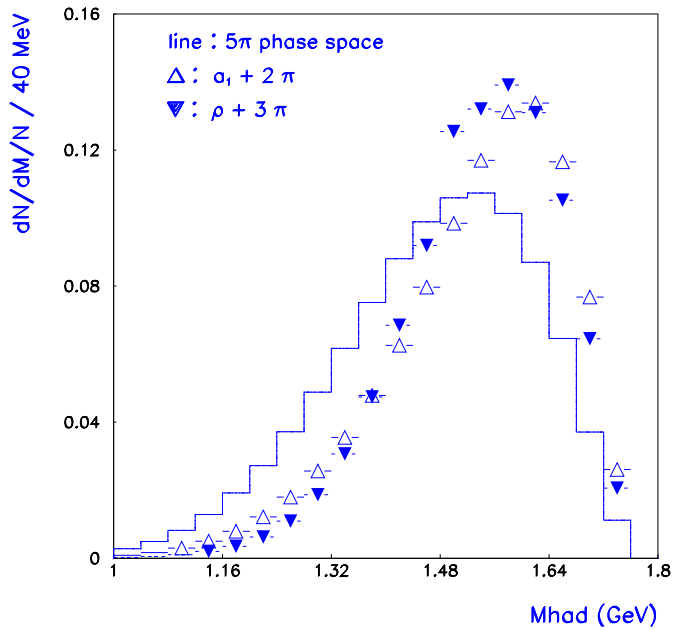

Figure 3: Invariant mass distribution of the 5π system for three assumptions on resonance production.
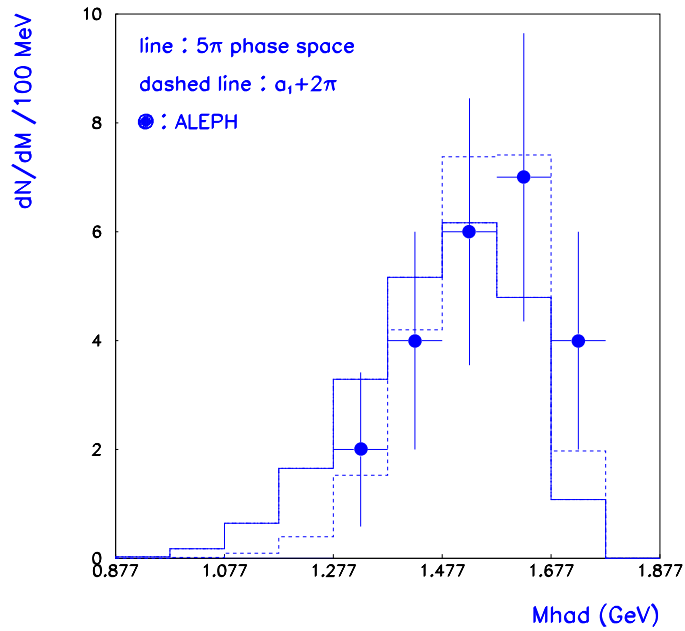
Figure 4: Invariant mass distribution of 5π data events compared with two assumptions on resonance production.
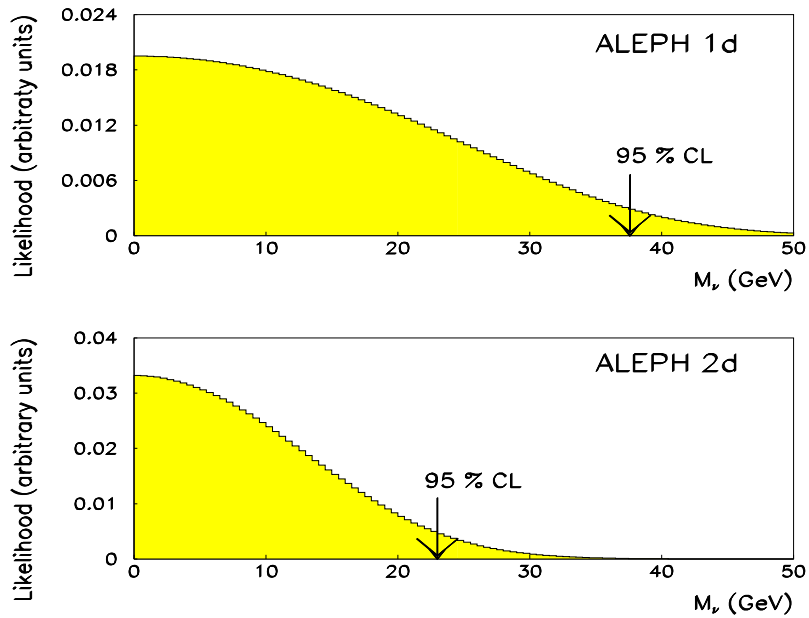

Figure 5: Total likelihood versus tau neutrino mass for the one dimensional (above) and two dimensional (below) fit.